ACS APPLIED MATERIALS & INTERFACES

Research Article

www.acsami.org

Universal Metal-Semiconductor Hybrid Nanostructured SERS Substrate for Biosensing

Soumik Siddhanta,[#,¶] Varun Thakur,[#,¶] Chandrabhas Narayana,*[,#] and S. M. Shivaprasad*[,#]

[#]Chemistry and Physics of Materials Unit, Jawaharlal Nehru Centre for Advanced Scientific Research, Jakkur P.O., Bangalore 560064, India

Supporting Information

ABSTRACT: We demonstrate here a novel high surface area GaN nanowall network substrate with plasmonic Ag nanodroplets, that can be employed as a highly sensitive, reproducible, and charge independent SERS substrate. The uniformity of the size and distribution of the Ag droplets and the absence of linker ligands result in large near-field intensity, while the GaN nanowall network morphology provides multiple reflections for signal enhancement. FDTD calculations simulate the observed hot-spot distribution and reiterate the higher performance of this hybrid substrate over conventional ones. Our studies on oppositely charged proteins provide a proof of concept for employing this as a versatile charge independent label free SERS substrate for trace biomolecule detection.

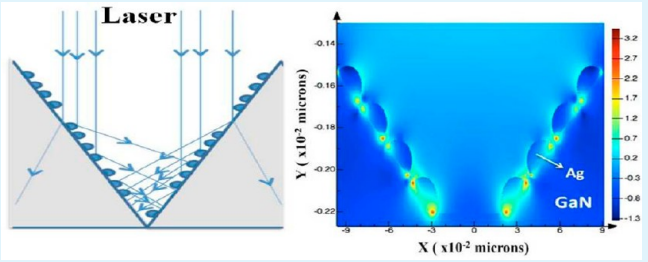

KEYWORDS: *surface enhanced Raman spectroscopy, GaN nanowall network, plasmonics, FDTD, biomolecule sensing (proteins)*

INTRODUCTION

Metallic nanostructures along with their semiconductor and dielectric counterparts have dominated the field of nanophotonics in the past decade. The ability to tailor-make their dimensions, organization, and properties in the nanoscale has ushered in miniaturization of novel devices. Nanoscale metallic structures can trap incident light through their surface plasmons and confine it to subwavelength spaces. These large field intensity enhancement and localization can be controlled by tailoring the shape, size, and distribution of the metallic nanostructures. Several techniques have been developed to exploit this unique light controlling ability at the nanoscale, and one of them is Surface Enhanced Raman Spectroscopy (SERS). When a molecule lies in the vicinity of a metal nanostructure, the surface plasmon-polariton that is generated when a laser source interacts with the substrate gives rise to SERS wherein the Raman scattering cross section can increase by as high as 10^{15} times.[1,2] The strong electromagnetic coupling among adjacent nanostructures results in areas of intense electromagnetic field called the "hotspots",[3,4] which yield greater SERS enhancement.

In recent times, SERS is emerging as a powerful tool for obtaining ultrasensitive vibrational spectra of molecules.[5−8] To exploit the full potential of SERS for a variety of applications, a large number of plasmonic substrates have been fabricated. Apart from colloidal substrates in the solution phase, solid SERS substrates have been fabricated by forming clusters or islands of metal nanostructures[9,10] and nanostructured films.[11] Recently, three-dimensional (3D) nanostructures such as porous substrates,[12] tips,[13] channels,[14] wires, etc. have been fabricated by employing electron beam lithography,[15] electroless deposition,[16] nanosphere lithography,[17] etc. Although sophisticated nanoscale patterning techniques have enhanced the versatility of this technique, it is plagued with issues of lack of reproducibility and reduction in the enhancement factor arising due to several reasons such as inhomogeneous attachments, variable particle distribution, charge selectivity, etc. When colloidal nanoparticles are employed, the capping agent forms a barrier between the nanostructure and the analyte molecule leading to decreased enhancement and unwanted background signal. In addition to reproducibility, a biochemical sensor demands the fabrication of a large surface area substrate with a uniform enhancement factor. Therefore, a uniformly distributed plasmonic nanostructure on a substrate would be ideal for use as a SERS substrate. Apart from the plasmonic nanostructures, it has been previously observed that the underlying substrate also plays an important role in the SERS enhancing capability.[18] The surface plasmons of the nanomaterials are known to be directly influenced by the physical environment, since the incident electromagnetic field induces charge polarization on the nanodroplets which is affected by that of the substrate and results in a shift in the surface plasmon resonance.[19] Formation of regions of high electric field intensities similar to hotspots between a metal coated nanowire and a dielectric substrate was reported by Glembocki et al.[20] Plasmonic nanostructures on dielectric films have also been observed to induce optical interference based enhancement of SERS.[21] Thus, it is worthwhile to tailor-make

Received: July 16, 2012
Accepted: October 8, 2012
Published: October 8, 2012

SERS substrates of different nanoparticle-dielectric/semiconductor hybrid geometries that can enhance SERS signals.

In this paper, we report a novel metal-semiconductor hybrid three-dimensional GaN nanowall structure as a substrate, where silver nanodroplets were deposited by physical vapor deposition. The plasmonic nanodroplets thus formed were not stabilized by any external chemical capping agent and yielded signals with a high degree of reproducibility and no background signal. The veracity of this novel substrate was tried by SERS experiments conducted on proteins of both positive and negative charges to evaluate the universal nature of the substrate, since it has been difficult to get SERS of all proteins using a single substrate. By finite-difference-time-domain (FDTD) simulations, we demonstrate the higher near-field intensity in the vicinity of the Ag nanodroplets over GaN and compared this with the conventional silicon substrate, both in flat and in the nanowall configuration.

EXPERIMENTAL SECTION

The GaN nanowall network structure was grown on a c-plane sapphire substrate using molecular beam epitaxy (MBE) system (SVT Assoc.) in nitrogen rich conditions at 630 °C substrate temperature. The experimental setup, conditions, and growth details are described elsewhere.[22,23] Thin film of 0.6 μm thickness consists of a hexagonal network matrix with wedge-shaped nanowalls which have a thickness of about 150 nm at the bottom and taper to less than 10 nm at their apex with void regions of ≈200 nm between the walls. Electron beam evaporation was used to deposit the Ag (99.99% pure wire from Alfa Aeser) nanodroplets in a physical vapor deposition system with a base pressure of 1.0×10^{-9} Torr, on top of the MBE grown GaN nanowall network. The schematic diagram showing the steps of substrate fabrication is shown in Figure 1. FESEM was performed using FEI (Nova-Nano SEM-600) to image the substrate. X-ray photoelectron spectroscopy (XPS) was performed on all the samples using an instrument from Omicron to confirm the presence of Ag on the surface of the GaN substrate. Mg K_α rays were used with pass energy of 25 KeV to obtain the general scan. The Raman and the SERS spectra were recorded in the 180° backscattering geometry, using a 532 nm excitation from a diode pumped frequency doubled Nd:YAG solid state laser (model GDLM-5015 L, Photop Suwtech Inc.) and a custom-built Raman spectrometer equipped with a SPEX TRIAX 550 monochromator and a liquid nitrogen cooled CCD (Spectrum One with CCD 3000 controller, ISA Jobin Yvon).[24] Laser power at the sample was ≈8 mW, and a typical spectral acquisition time was 30 s. Before acquiring SERS spectra the substrate was immersed in the aqueous solution of analyte (both thiophenol and protein) for a minimum of 4 h and dried.

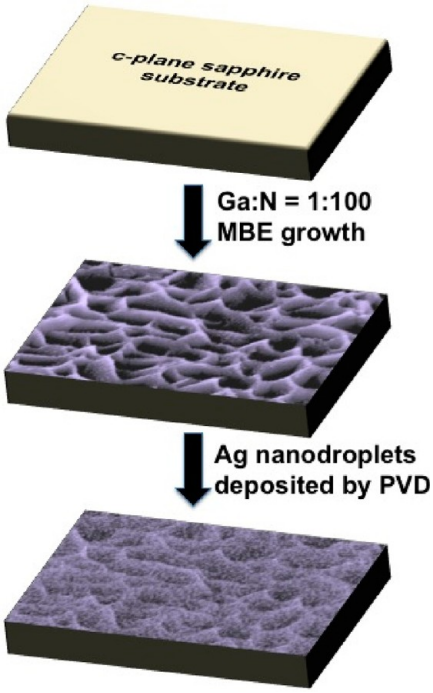

Figure 1. Schematic route for preparation of a high surface area GaN nanowall network substrate with plasmonic Ag nanodroplets.

Finite-Difference Time Domain (FDTD) Simulations: 2D FDTD simulations (Lumerical Solutions Ltd.) were used to determine the near-field intensities around the silver nanodroplets deposited over the GaN substrate. The simulation zone consists of periodic boundary conditions along the *x*-axis and along the *y*-axis, perfectly matched layers (PML) which absorb the waves moving out of the zone and hence preventing the reintroduction of reflections. Electromagnetic field distribution was calculated for silver nanodroplets with a radius of 10 nm and interdroplet separation of 5 nm, on a GaN layer for a planar surface and for a triangular nanowall configuration. A plane wave polarized light of wavelength 532 nm was used along the *y*-axis. For minimum simulation time and to maximize field enhancement resolution, the mesh override region was set to 0.5 nm, and the overall simulation time was 100 fs.

RESULTS AND DISCUSSION

Growing GaN on a c-plane Al_2O_3 (0001) surface in a nitrogen rich (Ga:N = 1:100) ambient atmosphere yields a self-assembled GaN nanowall network structure, to relax the lattice-mismatch strain at the interface. Nucleation at the edge dislocations results in the formation of the network matrix with wedge-shaped nanowalls,[22,23] which have a thickness of about 150 nm at the bottom and taper to less than 10 nm at the top. These walls surround open screw dislocations resulting in a very high surface area and are seen by XRD to be defect free wurtzite single crystals showing a strong band-edge PL peak at 362 nm with no defect emission.[23] Though conventionally, flat surfaces have been used to deposit metal nanoparticles for SERS applications, a corrugated dielectric or semiconductor surface can provide two important possibilities: a) nanoparticle-substrate interaction with a very high contact angle and b) a large surface area, with high density of nanoparticles that can result in the enhancement of SERS intensity. Ag deposited on these well structured surfaces is uniformly distributed as spherically shaped Ag nanodroplets of size ≈20 nm, with an interparticle spacing of ≈5 nm (Figure 2). The PVD method to grow Ag on GaN nanowalls yields very clean samples, and it is also compatible with MBE growth (can be integrated in one system) and does not use stabilizing surfactants or capping layers.

Energy dispersive X-ray analysis (EDAX) and XPS was done on the sample to confirm that the droplets are made of Ag. There is also an evidence of formation of oxide on the silver nanodrop surface as evident from the XPS study (Figure S1). To demonstrate the effectiveness of this GaN nanowall − Ag nanodroplet configuration for SERS, we have compared similar experiments performed on commercial GaN epilayer (2 μm flat film), on Al_2O_3 (0001). Ag did not adsorb well on the c-plane GaN thin flat film, and its adherence was weak and patchy. Figure 3 shows the SERS enhancement of thiophenol adsorbed on the silver nanodroplets-GaN substrate and a significantly lower signal on the 2D flat epilayer. Thiophenol was used to calculate the SERS enhancement factor (G), by the method given by Yu et al.[25]

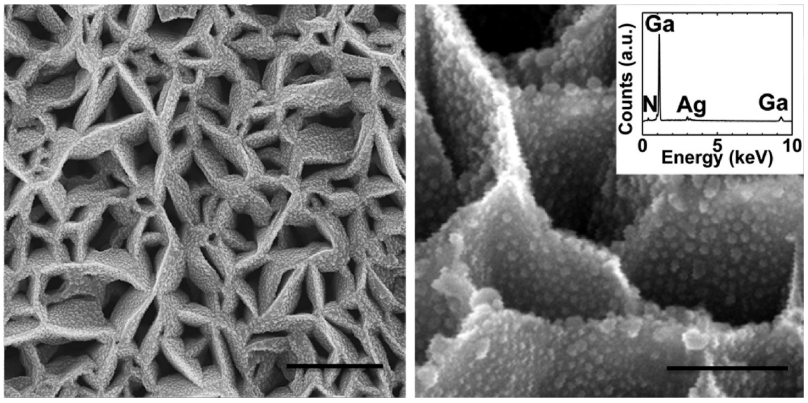

Figure 2. FESEM images of the 3D GaN nanowall substrate with silver nanodroplets deposited on them. The average size of the Ag nanodroplets was 20 nm with an average interparticle distance of 5 nm. The scale bars correspond to 500 nm (left) and 100 nm (right). The inset shows the EDAX of the substrate to confirm the presence of silver.

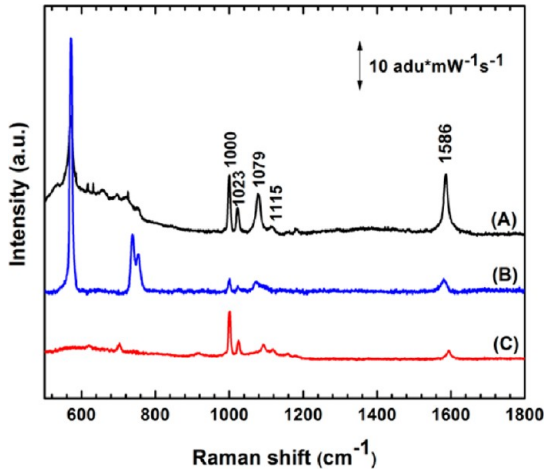

Figure 3. SERS spectra of (A) 1 mM thiophenol on the silver nanodroplets coated GaN nanowall substrate, (B) 1 mM thiophenol on the silver deposited GaN epilayer. (C) shows the normal Raman spectra of neat thiophenol using 532 nm wavelength laser. Note that below 800 cm^{-1} Raman spectrum is dominated by GaN related features.

$$G = (I_{SERS}/I_{NORM})(N_{BULK}/N_{SURF})$$

where I_{SERS} and I_{NORM} are the intensities of a specific band in SERS and normal Raman of the analyte molecule, respectively. N_{BULK} and N_{SURF} are the number of probe molecules which are illuminated under the laser beam in bulk and SERS experiments, respectively. N_{SURF} is given by CA, where C and A are the surface densities of thiophenol (6.8×10^{14} molecules cm^{-2}) and the laser spot area, respectively.[26] N_{BULK} is given by $Ah\rho/m$, where h, ρ, and m are the penetration depth (100 μm), the density (1.079 g cm^{-3}), and the molecular weight (110.18 g mol^{-1}) of thiophenol, respectively. The typical enhancement factor (EF) calculated for this substrate is 10^5. The stable SERS spectra of thiophenol is due to the binding of the thiol group to the silver nanoparticle surface, which corroborates with the frequency of the in-plane breathing mode coupled to the ν(C−S) mode decreases from 1092 to 1069 cm^{-1}.[27] This EF is comparable to the values in earlier reports of Ag nanoparticles on GaN substrates.[28] Since the nanodroplets are separated by a gap of 5 nm, which is much more than required for creating hotspots of intense electromagnetic field, leading to EF a few orders of magnitude lower than that of other silver nanostructures reported in the literature successful in ultratrace detection of small molecules or Raman reporter molecules.[29−32] This is a trade-off considering that a gap of 5 nm between the nanodroplets is beneficial in obtaining spectra of large molecules like proteins which is demonstrated in this paper. The high sensitive silver nanostructure reported earlier[29−32] have not demonstrated SERS of proteins, presumably, because the hotspot regions are much less than sizes of the proteins used here.

The supporting substrate for metallic nanoparticles plays an important role in the surface plasmon resonance (SPR) of the nanoparticles. Charge polarization of the metal-semiconductor/dielectric system under external electromagnetic field affects the SPR of the nanoparticles.[19] The nanoparticle-semiconductor junction might also lead to Schottky barrier formation which is not very large in our case due to small Ag clusters not covering the surface fully.[33] However, the barrier, if any, is not expected to affect SERS enhancement.[34] The SERS enhancement is explained from the electromagnetic field distribution around the nanodroplets deposited on the GaN substrate (shown in Figure 4). The Ag deposited GaN nanowall substrate showed highest electric field strength $|E|^2$ of 2829.4 which is about 3 times more than that for Ag deposited on the flat GaN substrate as calculated by FDTD simulation. Larger near-field intensity in the case of GaN is observed in comparison to silicon, which shows a maximum field intensity of 1.32 in the vicinity of silver nanodroplets adsorbed on a flat layer. Since the SERS enhancement factor is given by $|E|$,[4] its values depend on the near-field intensity in the vicinity of the nanodroplets. The near-field intensities are influenced as the incoming electromagnetic field experiences a change in dielectric constant due to the presence of the dielectric or semiconductor substrate, causing a change in the distribution of the electric field in the vicinity of the nanodroplets.[19] The electric field is focused in definite regions between the nanoparticle-dielectric junctions giving rise to active sites for SERS enhancement.[20] In the nanowall configuration the greater field intensity can be attributed to the increased focusing effect of the denser GaN substrate or to the multiple reflections that the incoming radiation suffers inside the cavity surrounded by the nanowalls. The calculations also show that silver nanoparticles grown on the GaN substrate have better SERS enhancement than on traditionally used substrates like silicon. Thus the GaN nanowall/Ag substrate has several advantages over other pristine metal nanoplates that have been grown on semi-

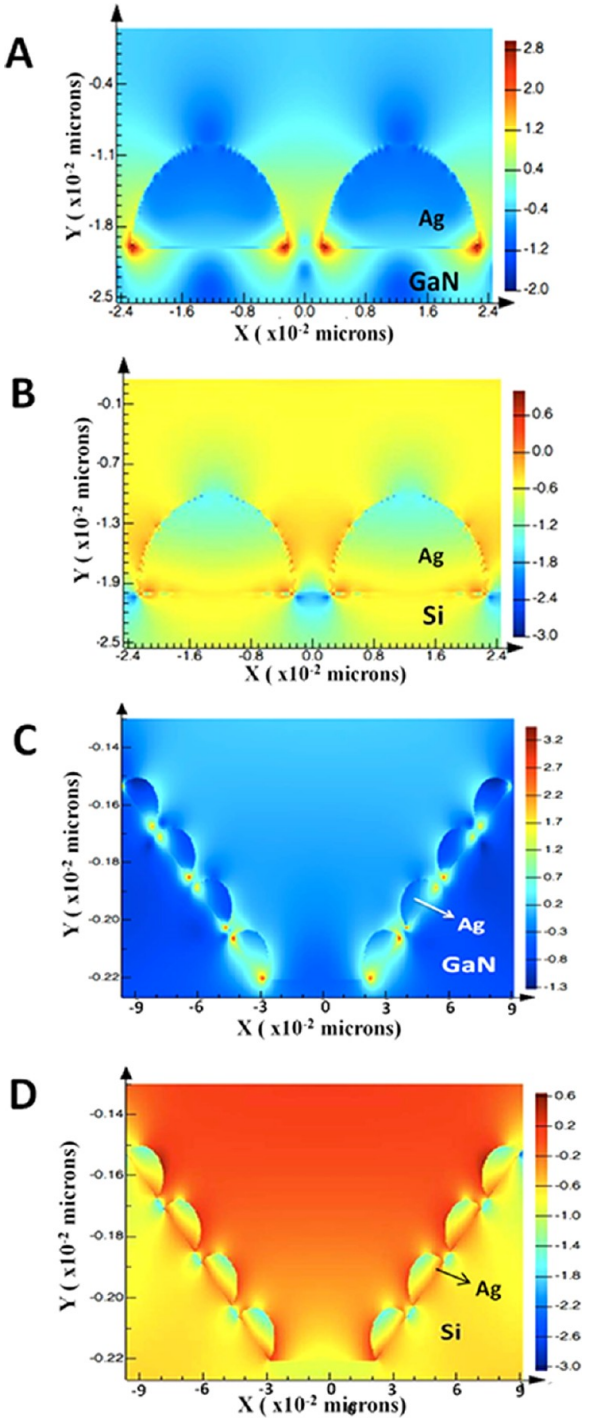

Figure 4. E-field amplitude patterns obtained from 2D FDTD calculations at wavelength 532 nm of silver nanodroplets on (A) a flat GaN layer, (B) a flat silicon layer, and (C) a GaN nanowall surface with 200 nm diameter pit and walls with a maximum thickness of 150 nm and (D) a silicon surface with similar morphology as C. The background material was taken as air with $n = 1$.

conductor substrates having high reflectivity[35,36] since it is difficult to maneuver the nanoplates to introduce multiple reflections or to control their orientation and introduce uniform surface distribution.

Another important aspect of the silver nanodroplet decorated GaN substrate is the reproducibility of SERS signals shown in Figure 5. SERS spectra obtained from nine different regions of

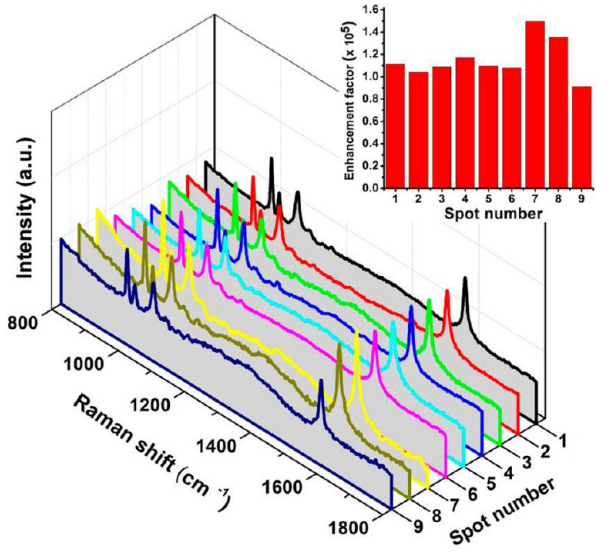

Figure 5. SERS spectra of 1 mM thiophenol on randomly selected nine spots of the silver deposited GaN nanowall substrate, demonstrating signal uniformity and reproducibility.

the single substrate of size 2 mm × 2 mm showed good reproducibility with the little fluctuations in the enhancement factors coming from reminiscent thiophenol molecules in the cavities. Conventionally, SERS is marred by the problem of reproducibility since analyte signals show large fluctuations in the enhancement factor due to irregular hot spot distribution. The uniform distribution of the nanodroplets leads to uniformity of hotspots resulting in high reproducibility.[37] Since the enhancement factor depends upon the particle size of the silver nanostructure we have also fabricated different sized nanodrops by annealing the substrate to 600 °C and also by depositing more silver by PVD. As indicated in Figure S2, although the enhancement increases by an order of magnitude, the substrate shows poor reproducibility of SERS spectra (showing a larger variation in the enhancement factor) over a large sample area, which is due to the inhomogenity in the size of the formed silver nanostructures. Therefore, in the present study, we chose the substrate with silver nanodroplets of 20 nm in diameter which are uniformly deposited on the GaN substrate, resulting in a uniform SERS enhancement over the entire surface area. This has a major advantage, especially when one tries to pattern the substrate for multiparameter detection. The roughness of the GaN substrate also plays an important role in preventing the "coffee ring effect" in which the analyte molecules on drying of the solution are deposited on the droplet edge leading to uneven distribution.[37] This also happens in the case of colloidal nanoparticles when they are mixed with the analyte molecules and deposited on a surface to obtain SERS spectra. In the GaN nanowall substrate, the rough surface with hollow cavities prevents the molecules from escaping to the edges on drying and therefore ensures even distribution. This has been demonstrated with a much mobile and small molecule thiophenol which shows uniform reproducibility in SERS spectra. The differential reflectivity due to the nonuniform nanoparticle aggregates also leads to nonuniform optical reflectivity causing irreproducible SERS.[38] Since the nanodroplets are firmly supported by the GaN substrate, there is no analyte induced aggregation taking place, and therefore the reproducibility of the substrate is maintained.

SERS is emerging as a powerful tool in bioanalysis as it provides information about the secondary structure of protein and can detect protein drug interactions.[39−41] In the past, we have carried out SERS of biologically important proteins like Coactivator-Associated Arginine Methyltransferase and Human transcriptional coactivator p300.[42,43] Protein-small molecule interactions were also investigated to understand the effect of inhibitors and activators of the proteins.[44,45] It should be noted that attachment of different proteins to SERS active substrates has always been challenging since the capping agent stabilizing the nanoparticle poses as a barrier for the protein to directly attach to the nanoparticle surface (for e.g. PCAF, which is also a transcriptional coactivator like p300 failed to give SERS signal with citrate capped colloidal silver nanopaticles). Therefore, one of the most difficult aspects of using SERS in proteins is that most of the substrates are selective to a particular type of protein only. Obtaining good and reproducible SERS spectra of proteins is most difficult among all other biomolecules. The diverse surface groups, properties, different shapes and sizes, and different manner of interaction with the nanostructure surface make the development of a universal substrate very difficult for proteins.[46] In view of this, developing a versatile SERS substrate for studying proteins of different charges is important and will have a strong impact in the field of drug development. Proteins are constituted by the zwitterionic amino acids, which are connected by peptide bonds, and therefore based on the composition; it may have a net charge, positive, negative or be charge neutral. In order to demonstrate the universality of the SERS substrate we have shown here the SERS spectra of two oppositely charged proteins, Human Serum Albumin (HSA, pI of 5.5 in neutral pH) and lysozyme (pI of 11 in neutral pH) (Figure 6), obtained on the Ag/GaN substrates. Both of these proteins are bigger molecules with diameters of a few nanometers (HSA molecule in solution is an ellipsoid of around 11 nm in length[47]). Therefore protein molecules lying away from the hotspot might not give good SERS signals and can lead to background fluorescence. The average of 5 nm gaps between the nanodroplets allows the protein to settle between the hotspots and give reasonable SERS enhancement for sensing purposes. Proteins interact with nanostructures using adsorption with or without electrostatic attraction or form covalent bonds through cysteine-like moieties. In the present case it is purely adsorbed on the Ag nanodroplets. In our earlier studies on P300[42] and CARM1[43] proteins we have demonstrated that the protein activity is retained even in the presence of silver nanoparticles, hence the protein structures do not undergo large scale changes.

The observed bands can be assigned to the proteins based on those reported in the literature.[48,49] It should be noted that many of the bands of the SERS spectra of proteins differ on changing the nature of the nanostructure, as the orientation and attachment region of the protein to the nanostructure change. The spectra of the proteins are dominated by the amide bands which provide information about the secondary structure of the protein and the bands corresponding to the aromatic amino acids. The spectra also contain modes corresponding to backbone chain vibrations. In the case of lysozyme the amide II and III modes can be seen at 1540 cm^{-1} and 1261 cm^{-1}, respectively, while the prominent amide I band is either absent or dominated by bands from other aromatic amino acids. The bands at 887, 1004, 1359, and 1583 correspond to aromatic amino acids like phenylalanine, tyrosine, and tryptophan. In HSA, the amide I, II, and III bands can be seen at 1615, 1520,

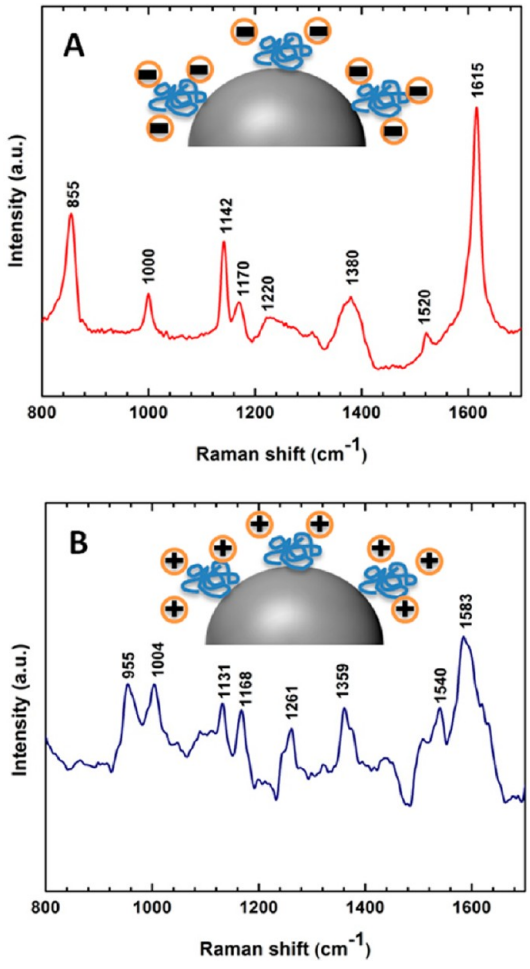

Figure 6. SERS spectra of proteins (A) 10^{-5} M Human Serum Albumin and (B) 10^{-5} M lysozyme, demonstrating charge independent detectability of the substrate.

and 1220 cm^{-1}, while the aromatic amino acid bands lie at 855 and 1000, respectively. Some of the aromatic amino acid bands overlap with the amide bands of the proteins. In most cases, proteins have a set of SERS bands which are distinct from each other as shown in the spectra of lysozyme and HSA. This presents a proof of principle that proteins can be differentiated and can be detected by SERS using similar sample preparation techniques for differently charged proteins and with limited knowledge about the nature of the proteins using the GaN nanowall based plasmonic substrate.

CONCLUSION

In conclusion, we have shown that a novel 3D SERS substrate was fabricated by using a hybrid physical method by depositing silver nanodroplets over a GaN nanowall substrate. The GaN nanostructure stabilizes the nanodroplets avoiding aggregation related problems, yielding highly reproducible results in SERS applications. The morphology of the substrate enabled multiple reflections in the nanowall cavity leading to enhancement of SERS signals. FDTD simulations show that GaN with noble metal nanostructures have superior electric field enhancement than conventional substrates like silicon. It was shown that this kind of bare and clean nanostructure can be used for sensing and distinguishing between complex biomolecules such as proteins irrespective of their charge in label free method. Thus,

these kinds of GaN based plasmonic substrates promise to be attractive prospects for protein diagnostics and other bioanalytical applications. This proof of concept is being followed by experiments to form more symmetric nanowall structures and monodispersed Ag adsorbate droplets to understand the underlying mechanism better.

■ ASSOCIATED CONTENT

Ⓢ Supporting Information

XPS data and SERS spectra and enhancement factor of substrates with different silver nanoparticles coverage. This material is available free of charge via the Internet at http://pubs.acs.org.

■ AUTHOR INFORMATION

Corresponding Author

*E-mail: cbhas@jncasr.ac.in (C.N.), smsprasad@jncasr.ac.in (S.M.S.).

Author Contributions

¶These authors contributed equally. The manuscript was written through contributions of all authors. All authors have given approval to the final version of the manuscript.

Notes

The authors declare no competing financial interest.

■ ACKNOWLEDGMENTS

S.M.S. thanks Prof. C. N. R. Rao for his support and guidance. The authors acknowledge Manoj Kesaria for providing the samples. S.S. and V.T. would like to acknowledge JNCASR for scholarships.

■ REFERENCES

(1) Du, L.; Zhang, X.; Mei, T.; Yuan, X. *Opt Express* **2010**, *18*, 1959–65.
(2) Agarwal, G. S.; Jha, S. S.; Tsang, J. C. *Phys. Rev. B* **1982**, *25*, 2089–2093.
(3) Alonso-González, P.; Albella, P.; Schnell, M.; Chen, J.; Huth, F.; García-Etxarri, A.; Casanova, F.; Golmar, F.; Arzubiaga, L.; Hueso, L. E; Aizpurua, J.; Hillenbrand, R. *Nat Commun.* **2012**, *3*, 684.
(4) Stranahan, S. M.; Willets, K. A. *Nano Lett.* **2010**, *10*, 3777–84.
(5) Kneipp, J.; Kneipp, H.; Kneipp, K. *Chem. Soc. Rev.* **2008**, *37*, 1052–1060.
(6) Hering, K.; Cialla, D.; Ackermann, K.; Dörfer, T.; Möller, R.; Schneidewind, H.; Mattheis, R.; Fritzsche, W.; Rösch, P.; Popp, J. *Anal. Bioanal. Chem.* **2008**, *390*, 113–124.
(7) Aroca, R. *Surface-Enhanced Raman Spectroscopy*; Wiley: New York, 2006.
(8) Kneipp, K.; Moscovitz, M.; Kneipp, H. Surface Enhanced Raman Spectroscopy: Physics and Applications. *Topics in applied physics*; Springer.
(9) Yuan, W.; Ho, H. P.; Lee, R. K.; Kong, S. K. *Appl. Opt.* **2009**, *48*, 4329–37.
(10) Aroca, R.; Martin, F. *J. Raman Spectrosc.* **1985**, *16*, 156–162.
(11) Brayner, R.; Iglesias, R.; Truong, S.; Beji, Z.; Felidj, N.; Fiévet, F.; Aubard, J. *Langmuir* **2010**, *26*, 17465–9.
(12) Lu, L.; Eychmüller, A.; Kobayashi, A.; Hirano, Y.; Yoshida, K.; Kikkawa, Y.; Tawa, K.; Ozaki, Y. *Langmuir* **2006**, *22*, 2605–9.
(13) Linn, N. C.; Sun, C. H.; Arya, A.; Jiang, P.; Jiang, B. *Nanotechnology* **2009**, *20* (22), 225303.
(14) Ko, H; Tsukruk, V. V. *Small* **2008**, *4*, 1980–1984.
(15) David, C.; Guillot, N.; Shen, H.; Toury, T.; de la Chapelle, M. L. *Nanotechnology* **2010**, *21* (47), 475501.
(16) Bhuvana, T.; Kumar, G. V. P.; Narayana, C.; Kulkarni, G. U. *Nanotechnology* **2007**, *18*, 145702.
(17) Dick, L. A.; McFarland, A. D.; Haynes, C. L.; Van Duyne, R. P. *J. Phys. Chem. B* **2002**, *106*, 853–60.
(18) Kudelski, A.; Pisarek, M.; Roguska, A.; Hołdyński, M.; Janik-Czachor, M. *J. Raman. Spectrosc.* **2009**, *40*, 1652–1656.
(19) Noguez, C. *J. Phys. Chem. C* **2007**, *111*, 3806–3819.
(20) Glembocki, O. J.; Rendell, R. W.; Alexson, D. A.; Prokes, S. M.; Fu, A.; Mastro, M. A. *Phys. Rev. B* **2009**, *80*, 085416.
(21) Shoute, L. C. T.; Bergren, A. J.; Mahmoud, A. M.; Harris, K. D.; McCreery, R. L. *Appl. Spectrosc.* **2009**, *63*, 133–140.
(22) Kesaria, M.; Shetty, S.; Shivaprasad, S. M. *Cryst. Growth Des.* **2011**, *11* (11), 4900–4903.
(23) Kesaria, M.; Shivaprasad, S. M. *Appl. Phys. Lett.* **2011**, *99*, 143105–3.
(24) Kumar, G. V. P.; Chandrabhas, N. *Curr. Sci.* **2007**, *93*, 778–781.
(25) Yu, H. Z.; Zhang, H. L.; Liu, Z. F. *Langmuir* **1999**, *15* (1), 16–19.
(26) McFarland, A. D.; Young, M. A.; Dieringer, J. A.; Van Duyne, R. P. *J. Phys. Chem. B* **2005**, *109* (22), 11279–85.
(27) Bryant, M. A.; Joa, S. L.; Pemberton, J. E. *Langmuir* **1992**, *8* (3), 753–756.
(28) Williamson, T. L.; Guo, X.; Zukoski, A.; Sood, A.; Diaz, D. J.; Bohn, P. W. *J. Phys. Chem. B* **2005**, *109*, 20186–20191.
(29) Chaney, S. B.; Shanmukh, S.; Dluhy, R. A.; Zhao, Y. P. *Appl. Phys. Lett.* **2005**, *87* (3), 3.
(30) Asiala, S. M.; Schultz, Z. D. *Analyst* **2011**, *136* (21), 4472–4479.
(31) Lee, S. J.; Morrill, A. R.; Moskovits, M. *J. Am. Chem. Soc.* **2006**, *128* (7), 2200–2201.
(32) Camden, J. P.; Dieringer, J. A.; Zhao, J.; Van Duyne, R. P. *Acc. Chem. Res.* **2008**, *41* (12), 1653–1661.
(33) Kumar, P.; Kumar, M.; Sivaprasad, S. M. *Appl. Phys. Lett.* **2010**, *97*, 122105.
(34) Wang, R.; Liu, D.; Zuo, Z.; Yu, Q.; Feng, Z.; Liu, H.; Xu, X. *J. Mater. Chem.* **2012**, *22*, 2410–2418.
(35) Sun, Y.; Pelton, M. *J. Phys. Chem. C* **2009**, *113* (15), 6061–6067.
(36) Sun, Y. *Adv. Funct. Mater.* **2010**, *20* (21), 3646–3657.
(37) Shen, X.; Ho., C.-M.; Wong, T.-S. *J. Phys. Chem. B* **2010**, *114* (16), 5269–5274.
(38) Lin, X. M.; Cui, Y.; Xu, Y. H.; Bin, R.; Tian, Z. Q. *Anal. Bioanal. Chem.* **2009**, *394*, 1729–1745.
(39) Siddhanta, S.; Narayana, C. *Nanomater. Nanotechnol.* **2012**, *2*, 1–13.
(40) Miškovský, P.; Jancura, D.; Sánchez-Cortés, S.; Kočišová, E.; Chinsky, L. *J. Am. Chem. Soc.* **1998**, *120* (25), 6374–6379.
(41) Jurasekova, Z.; Marconi, G.; Sanchez-Cortes, S.; Torreggiani, A. *Biopolymers* **2009**, *91*, 917–927.
(42) Kumar, G. V. P.; Reddy, B. A. A.; Arif, M.; Kundu, T. K.; Narayana, C. *J. Phys. Chem. B* **2006**, *110* (33), 16787–92.
(43) Kumar, G. V. P.; Selvi, R.; Kishore, A. H.; Kundu, T. K.; Narayana, C. *J. Phys. Chem. B* **2008**, *112* (21), 6703–7.
(44) Mantelingu, K.; Kishore, A. H.; Balasubramanyam, K.; Kumar, G. V. P.; Altaf, M.; Swamy, S. N.; Selvi, R.; Das, C.; Narayana, C.; Rangappa, K. S.; Kundu, T. K. *J. Phys. Chem. B* **2007**, *111* (17), 4527–34.
(45) Mantelingu, K.; Reddy, B. A.; Swaminathan, V.; Kishore, A. H.; Siddappa, N. B.; Kumar, G. V.; Nagashankar, G.; Natesh, N.; Roy, S.; Sadhale, P. P.; Ranga, U.; Narayana, C.; Kundu, T. K. *Chem. Biol.* **2007**, *6*, 645–57.
(46) Han, X. X.; Zhao, B.; Ozaki, Y. *Anal. Bioanal. Chem.* **2009**, *394*, 1719–1727.
(47) Kiselev., M. A.; Gryzunov, I. A.; Dobretsov, G. E.; Komarova, M. N. *Biofizika* **2001**, *46* (3), 423–427.
(48) Podstawka, E.; Ozaki, Y.; Proniewicz, L. M. *Appl. Spectrosc.* **2004**, *10*, 1147–56.
(49) Stuart, S.; Fredericks, P. M. *Spectrochim. Acta, Part A* **1999**, *55*, 1615–1640.